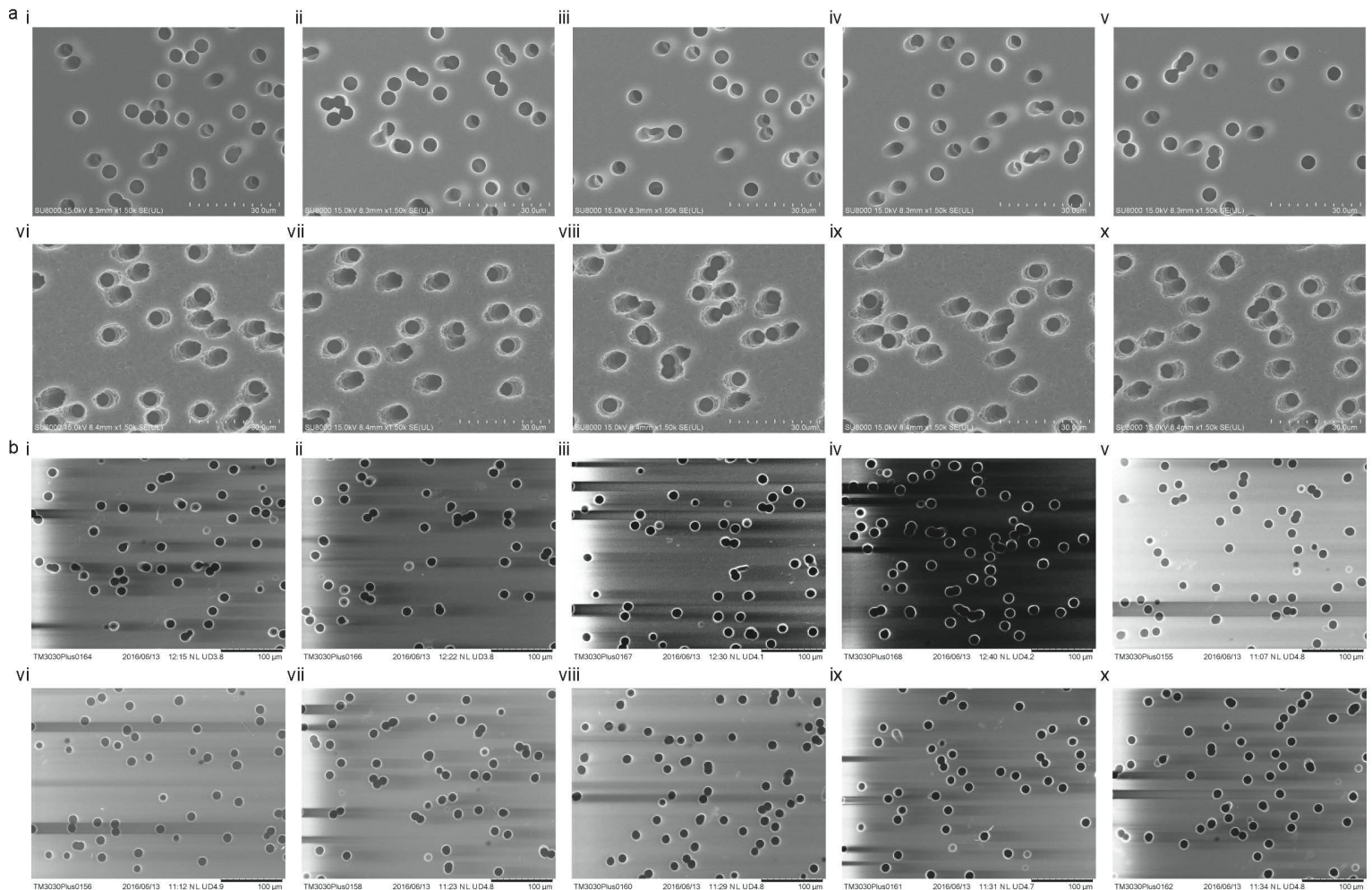
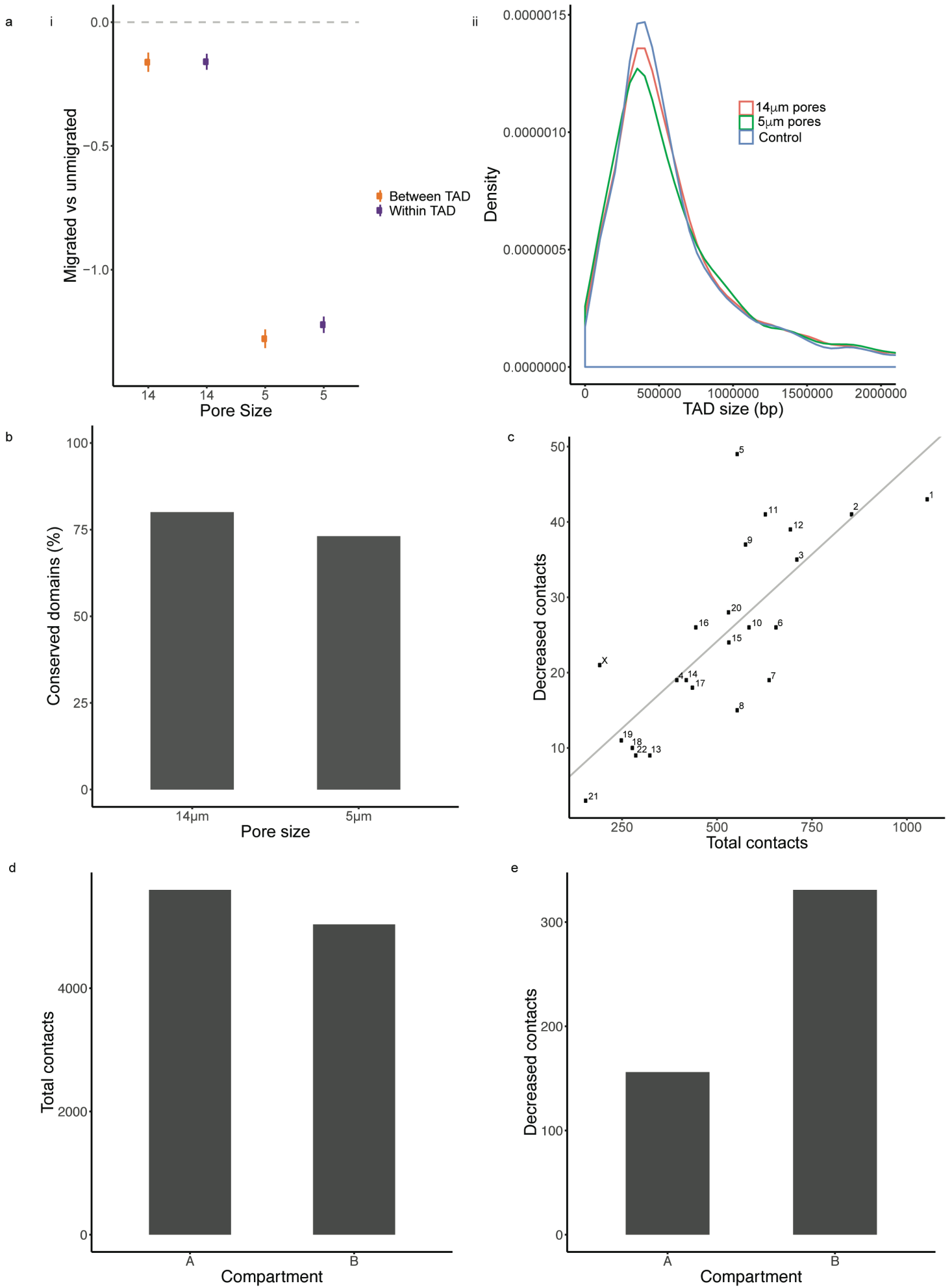


**Supplementary Figure 1.** *HL60 cells differentiated into neutrophil-like cells and migrated through two pore sizes.* a) Flow cytometry analysis of expression of the CD11b marker on HL60/S4 and HL60/S4-RA cells. HL-60/S4 cells treated with RA had higher levels of CD11b, indicating successful differentiation. Representative histogram shown. b) HL60 cells were cytopun onto microscope slides and Wright-Giemsa stained to compare nuclear morphology. Undifferentiated cells treated with vehicle (ethanol) for four days had spherical nuclei (i), while cells differentiated with retinoic acid for 4 days had lobed or partially lobed nuclei (ii). Representative images shown. c) Flow cytometry analysis of Alexa Fluor 488-annexin V and propidium iodide (PI) staining of live, dead and apoptotic cells following differentiation with retinoic acid (RA) (i) undifferentiated HL-60/S4 and (ii) differentiated HL-60/S4-RA cells. Over 85% of both HL-60/S4 and HL-60/S4-RA were viable. d) The JuliBr cell counting system (automated hemocytometer) was used to count and measure the diameter of cells in suspension. Cells were stained with trypan blue to

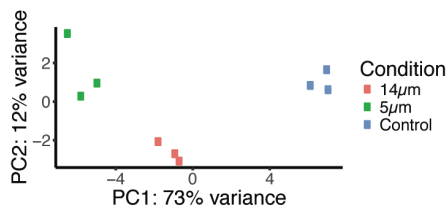
distinguish live and dead cells. Histogram shows mean count of cell diameters across 3 independent differentiation assays. Viable cells had an average diameter of  $6.99\ \mu\text{m}$  ( $\text{SD}=0.327$ ). e) Migration rate through  $5\ \mu\text{m}$  and  $14\ \mu\text{m}$  diameter pores. Cells were collected and processed every 30 minutes during the migration assay, and formaldehyde fixed cells were counted to assess migration rate. All time points were pooled per experiment, up to two experiments were pooled for Hi-C replicates of  $14\ \mu\text{m}$  pore migration, and up to four experiments were pooled for Hi-C replicates of  $5\ \mu\text{m}$  pore migration. Migration rates were consistent within and between replicates at each time point. Cells migrated more slowly through  $5\ \mu\text{m}$  pores when compared to migration through  $14\ \mu\text{m}$  pores, as they are required to remodel to fit through the smaller pore size.



**Supplementary Figure 2.** SEM of porous membranes. a) Scanning electron microscopy of the smooth (i-v) and rough (vi-x) sides of polycarbonate membranes with  $5\ \mu\text{m}$  diameter pores. a) Scanning electron microscopy of the rough (i-iv) and smooth (v-x) sides of polycarbonate membranes with  $14\ \mu\text{m}$  diameter pores. Although both membranes contained pores that were joined to make a larger single pore, the majority were joined at the edges and thus did not increase the minimum diameter of the pore.



**Supplementary Figure 3.** *Genome organisation changes after migration through two pore sizes.* a) Disruption of contacts occurred both within and between topologically associated domains (TADs). Contact frequency between upstream and downstream windows per bin (binsignal) as calculated by TopDom showed a statistically significant but small decrease after migration through 14 $\mu$ m pores, and a much larger decrease after migration through 5 $\mu$ m pores (Student's t test, all p values < 2.2e-16, difference in mean with 95% confidence displayed). b) TAD size and number was conserved in control, 5 $\mu$ m migrated, and 14 $\mu$ m migrated cells. c) Disrupted contacts were distributed across the genome. The number of disrupted contacts per chromosome correlates with the number of total significant contacts per chromosome ( $R^2 = 0.595$ ). d) A similar number of significant contacts were identified in compartment A and B (i) but twice as many of these contacts were disrupted in compartment B than A after migration through 5 $\mu$ m pores (ii).



**Supplementary Figure 4.** *RNA-seq PCA plot.* A) VST normalised RNA-seq results cluster by condition.

